Iranian Journal of Oil & Gas Science and Technology, Vol. 8 (2019), No. 3, pp. 18-39
http://ijogst.put.ac.ir

An Evaluation of Rock Integrity and Fault Reactivation in the Cap Rock and Reservoir Rock Due to Pressure Variations

Mohammad Abdideh* and Yaghob Hamid

Assistant Professor, Department of Petroleum Engineering, Omidiyeh Branch, Islamic Azad University, Omidiyeh, Iran
M.S. Student, Department of Petroleum Engineering, Omidiyeh Branch, Islamic Azad University, Omidiyeh, Iran

Received: January 13, 2019; *revised*: April 10, 2019; *accepted*: April 30, 2019

Abstract

Cap rocks are dams which can prevent the upward movement of hydrocarbons. They have disparities and weaknesses including discontinuities, crushed areas, and faults. Gas injection is an effective mechanism for oil recovery and pore pressure. With increasing pore pressure, normal stress is reduced, and the integrity of impermeable boundaries (cap rock, fault, etc.) becomes instable. A successful strategy for reservoir development is the inevitable necessity of conducting geomechanical studies and modeling the reservoir. The construction of a comprehensive geomechanical model, including the stress state is a function of depth (direction and amount), physical properties of the reservoir rock and its formations (rock resistance and elastic moduli), pore pressure estimation, and description and distribution of fractures and faults. In this work, analytical and numerical methods have been used in geomechanical modeling, and the data used for modeling and petrophysical information are downhole tests. The geomechanical modeling of gas injection into the reservoir and, simultaneously, the operation of Asmari reservoir and Marun oilfield cap rock in the southwest of Iran were carried out. The threshold of reactivating faults and the critical pressure of induced fracture were calculated, and the results were presented as analytical and numerical models. Moreover, in addition to analyzing the stress field at depths, the resistance parameters of the formations were determined. The results showed that the most changes and instabilities were around the wellheads, fractures, and the edges of the field.

Keywords: Cap Rock, Discontinuity, Gas Injection, Pore Pressure, Geomechanical Model, Elastic Rock Properties, Numerical Modeling

1. Introduction

Rock mechanics and geomechanics are among the sciences at the center of focus in studies related to the drilling, development, and exploitation of hydrocarbon fields around the world. The careful detection of in situ stresses across the fields and the different stresses applied to the environment surrounding wellbore via different processes, and combining these data with the mechanical parameters of common formations in hydrocarbon reservoirs comprise a key for addressing a wide range of costly

* Corresponding author:
Email: m.abdideh@yahoo.com

problems and issues in the oil industry. As far as designing hydraulic fracturing operation, well stability, and drilling programs are concerned, it is necessary to use geomechanical modeling. As such, geomechanical modeling plays an important role in cost reduction and the technical investigation of associated processes. In order to construct a geomechanical model, it is conventional to use data from porosity log, density log, sonic log, etc. along with the model calibrated using core analysis and well tests.

Actually, cap rocks can prevent the upward movement of hydrocarbons. Cap rocks are an impermeable set which generally depends on the thickness and height of the hydrocarbon column below it, and its lateral pressure and extension (Ansari et al., 2012). Gas injection is an effective mechanism for increasing oil extraction and pore pressure. In order to ensure the stability and consistency of impermeable boundaries (cap rock, fault, etc.), it is necessary to conduct geomechanical studies and analyses during production or gas injection to the reservoir (Han et al., 2012). The integrity of impermeable boundaries may be threatened or destroyed by induced fractures, activity, or reopening of faults and fractures present on the boundaries (Luiz Serra de Souza, 2012). Production from oil and gas reservoirs is accompanied by changes in geomechanical properties. These changes affect the state and amount of stress below the surface. The construction of a comprehensive geomechanical model including the stress state is a function of depth (direction and amount), physical properties of the reservoir rock and its formations (rock resistance and elastic moduli), pore pressure estimation, and description and distribution of fractures and faults (Akbar, 2005).

In general, first studies to evaluate the integrity of rocks during injection and production processes have been conducted over the last few years, of which the following can be mentioned.

The evaluation of rock continuity and the reactivation of faults by increasing pressure and thermal changes caused by CO_2 injection in a discharged gas field in the Netherlands and several other fields in Europe were studied using numerical and semi-analytic methods (Assef et al., 2010). In this research, with the aim of determining the maximum permissible injection pressure, geomechanical modeling was performed to investigate the effects of mechanical changes in porous, thermal, and chemical environments on the integrity of existing cap rocks and faults in relation to CO_2 storage. Then, the effects of mechanical changes in porous and thermal environments were studied by numerical methods, finite difference, and semi-analytical methods. Chemical effects were studied by a discrete element model.

The geomechanical analysis of rock integrity was carried out at the University of Saskatchewan, Canada in order to ensure the integrity of cap rocks oil recovery projects (CO_2 injection) during and after production and injection (Rivero, 2010).

In this study, semi-analytical and closed methods for determining the variation of induced stress during the variation of pore pressure in the reservoir and surrounding rocks were obtained under plain strain and axial symmetry conditions. Finally, the general patterns of induced stress variation, in-situ stress development, faults reactivation, and induced fractures were identified.

Because of the complex tectonic position of the Southwest oil fields of Iran in terms of creating faults and gaps, paying attention to these weaknesses in EOR processes becomes more important.

In this study, from the viewpoint of rock mechanics, the analytical and numerical modeling of geomechanics is discussed. The method is based on petrophysical data available in all wells.

The results show that, by using this method, the threshold of rock resistance and fault reactivity can be determined. It can greatly help design processes such as gas injection.

2. Geological setting

Marun oilfield is one of the largest oilfields in southern Iran located at 40 km east of Ahwaz and among Kupal, Aghajari, Ramin, Shadegan, and Ramshir fields (Figure 1). The length of the field at the head of the Asmari reservoir is about 67 km, and its width is about 7 km with a construction overhang of 2 km; the size of the reservoir at the head of the Daryan formation decreases to 60 km long and 5.3 km wide. The distance between the reservoir ridge and the deepest contact surface of water and oil in Asmari formation is about 2000 m.

Figure 1

Geographic location of Marun oilfield among Iran's oilfields (Abdideh and Hedayati Khah, 2017).

For modeling, data from the well in Marun oilfield were used. The depth of this well is 3872 m. The thickness of the Gachsaran formation in this well is 673 m and continues to a depth of 3657 m. The thickness of cap rock in this well is 65.5 m, which is under the layer 1 of Gachsaran formation, from the depth of 3591.5 to 3657; it is located at the top of Asmari formation, which is 215 m thick in this well. All petrophysical charts are taken from the ground to the bottom of the well. The availability of these diagrams is the basis of geomechanical studies and calculations.

Table 1 shows various types of lithology and the density of the layers of Gachsaran formation, which plays the role of cap rock in this field. According to this information, the largest volume of Gachsaran formation in this well consists of salt and marl units, which have plastic properties (Figure 2).

Table 1

Lithology and density related to the layers of Gachsaran formation in the studied wells.

Formation	Lithology	Density
Gachsaran 7	Made up of mainly anhydrite and some gray marl and limestone	**2.58<density<3.02**
Gachsaran 6	Mainly anhydrite, salt, red, and marl layers	**2.46<density<2.9**
Gachsaran 5	Mainly anhydrite, salt, red, and gray layers	**2.22<density<2.58**
Gachsaran 4	Mainly anhydrite, salt and gray marl layers	**2.5<density<2.97**
Gachsaran 3	Thick anhydrite with subordinate salt in the lower half, and alternating anhydrites, thin limestone and marls in the upper half	**2.46<density<2.94**
Gachsaran 2	Thick salt units with intervening anhydrite and thin limestone	**2.53<density<2.92**
Gachsaran 1 (Cap Rock)	Mainly anhydrite and gray marl and minor layers of limestone	**2.69<density<2.71**

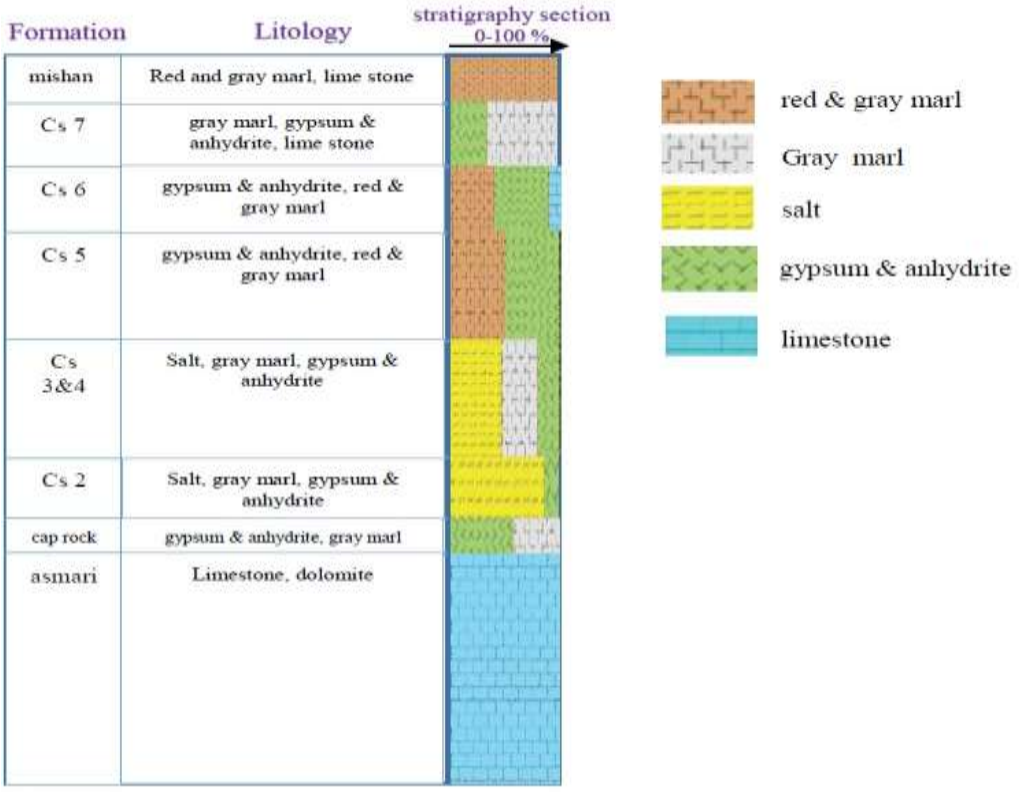

Figure 2

Alternation of anhydrite, salt, and marl in Gachsaran formation in one of the studied wells.

3. Materials and methods

According to the National Iranian Oil Company, a large number of Iranian oil reserves are in the second half of their lives, and a failure to inject gas into them on time will lead to a severe drop in pressure and recycling rates, resulting in the burial of a large part of the oil in these fields.

According to expert estimates, the injection of every one million cubic feet of natural gas into oil reservoirs would enhance oil recovery by an average of about 150 barrels of extra oil (Dutta, 2011). According to experts, in case of the optimization of gas consumption in the country and an increase in the share of gas injection into oilfields, while enhancing the rate of recovery of oil reservoirs, conditions

for gas exports will be provided in the coming decades. In fact, because in this process gas is stored in addition to increasing oil production, gas can be released in the future.

The injection of gas in the reservoir, which mainly aims at increasing the operation, may cause changes in the in situ stress field by changing pore pressure and reactivate discontinuities and create new discontinuities, which lead to induced seismic events and reduce the permeability capacity of cap rocks. Hence, the recognition of the geological and discontinuity features of the reservoir and cap rock is of particular importance in determining the safe interval of injection fluid pressure and injection site (Holland et al., 2010). In general, analyzing the issues and risks associated with gas injection from the geomechanical point of view includes two main steps: The first is to analyze the amount of stress variation by gas injection, and the second analyzes the behavior of geological indicators (reservoir and cap rock layers, fractures, faults, etc.) due to the stress induced (Archer and Rasouli, 2012). The production and injection of fluid, by changing the pore pressure and the corresponding variations in the stress field, may cause hydraulic failure and shear failure at the crack levels or may reactivate the existing discontinuities through effective stress reducing (Perfetto, 2013). Therefore, the deformation of the earth, earthquakes happened, the reactivation of discontinuities, and the permeability of the rocks surrounding the reservoir and cap rock are important factors in the implementation of projects involving gas injection into underground spaces.

The basis for assessing the resistance and integrity of cap rocks is the construction of a geomechanical well model and the analysis of these models.

The geomechanical model is a numerical representation of the state of in situ stresses and the mechanical properties of rock for a stratigraphic column in the field (Afsari et al., 2009). In general, the geomechanical model relates the properties of the dynamical elasticity of the formation to its equivalent static elastic properties, which are the properties of static elasticity to determine the resistance of the formation and the stresses in the ground. A geomechanical model consists of deep profiles including elastic or elasto-plastic parameters, rock resistance, in situ stresses in the ground, pore pressure, and the direction of in situ stresses of the ground (Fjaer et al., 2008).

Using petrophysical images and dipole shear imager (DSI) logs, mechanical parameters are estimated or determined and a geomechanical model is constructed. This model is more complete with new drill information and can be updated at any time (Khaksar et al., 2009). This type of model in oil and gas fields can be one-dimensional (in the direction of well drilling) and three-dimensional. In the following, we introduce a variety of geomechanical models.

3.1. One-dimensional geomechanical models

A one-dimensional geomechanical model is constructed based on the recorded data of well logs, including sonic logging (shear and compression wave), density, caliper, porosity, and gamma radiation, and it defines a section of depth against the mechanical properties and tensile stresses of the wall rocks and the rocks around the well. The one-dimensional geomechanical model is the basis for geomechanical analysis and the study of the effects of rock mechanics on the walls and around the wells and incidents such as wall collapsing, sand production, etc. (Chang and Zoback, 2006). A geomechanical one-dimensional model includes rock resistance (unenclosed pressure strength, tensile strength, and friction angle), deformation parameters (Young's modulus, Poisson's ratio, shear and bulk moduli), vertical and horizontal stresses, pore pressure, and necessary properties to predict sustainability (Zoback, 2007).

3.2. Three-dimensional geomechanical models

A three-dimensional geomechanical model, on the scale and dimensions of the total reservoir, field, or sedimentary basin, is the numerical representation of geomechanical parameters in three dimensions (Lee, 2013).

4. Results and discussion

As stated, the first step in assessing the integrity and resistance of underground formations is the construction of a well geomechanical model. In general, the stages of building a geomechanical model include:

1. Identification of formations based on their material; some formations have granular behavior (e.g. sandstone) and others show plastic behavior (e.g. shale). Thus, gamma logs can be used for this purpose.
2. Estimation of rock properties; this step involves estimating elastic properties (such as Young's modulus) and resistance properties (such as uniaxial compressive strength and tensile strength) and calibrating them based on laboratory results.
3. Calculation of stress field and pore pressure in the oil field; in this case, the vertical stress is obtained using a density log, and the horizontal stresses are then estimated.

4.1. Calculation of rock elastic modulus

The calculation of rock elastic modulus such as Young's modulus and Poisson ratio are the most fundamental part in underground stress analysis. The two modules are calculated using the following formula:

$$\vartheta dyn = \left(\frac{\frac{1}{2}\left(\frac{\mathrm{DTS}}{\mathrm{DTC}}\right)^2 - 1}{\left(\frac{\mathrm{DTS}}{\mathrm{DTC}}\right)^2 - 1}\right) \quad \text{Poisson ratio} \tag{1}$$

$$Edyn = RHoB \times {V_c}^2 \times \left(\frac{3{V_c}^2 - 4{V_s}^2}{{V_c}^2 - {V_s}^2}\right) \times (0.00030482) \times 10^2 \quad Young's\ modulus \tag{2}$$

where, V_c and V_s are the compressive and shear wave velocities; according to $\frac{\mathrm{Ft}}{\mu\mathrm{s}}$, DTC are the compressive and shear wave transfer time, and, according to $\mu\frac{\mathrm{s}}{\mathrm{Ft}}$, RHOB is the density of the rock.

The Poisson ratio and dynamic Young's modulus can be converted from empirical equations to static equations to become similar to those obtained from cores. One of these empirical equations is Wang's equation, which is used as a suitable method for converting dynamic values to static laboratory values (Eissa and Kazi, 1988).

$$\vartheta S = 0.7\vartheta dyn \tag{3}$$

$$E_{sta} = 0.4145E_{dyn} - 1.059 \tag{4}$$

Figure 3 shows the variation of the elastic moduli in relation to the depth in the cap rock of the studied oilfield.

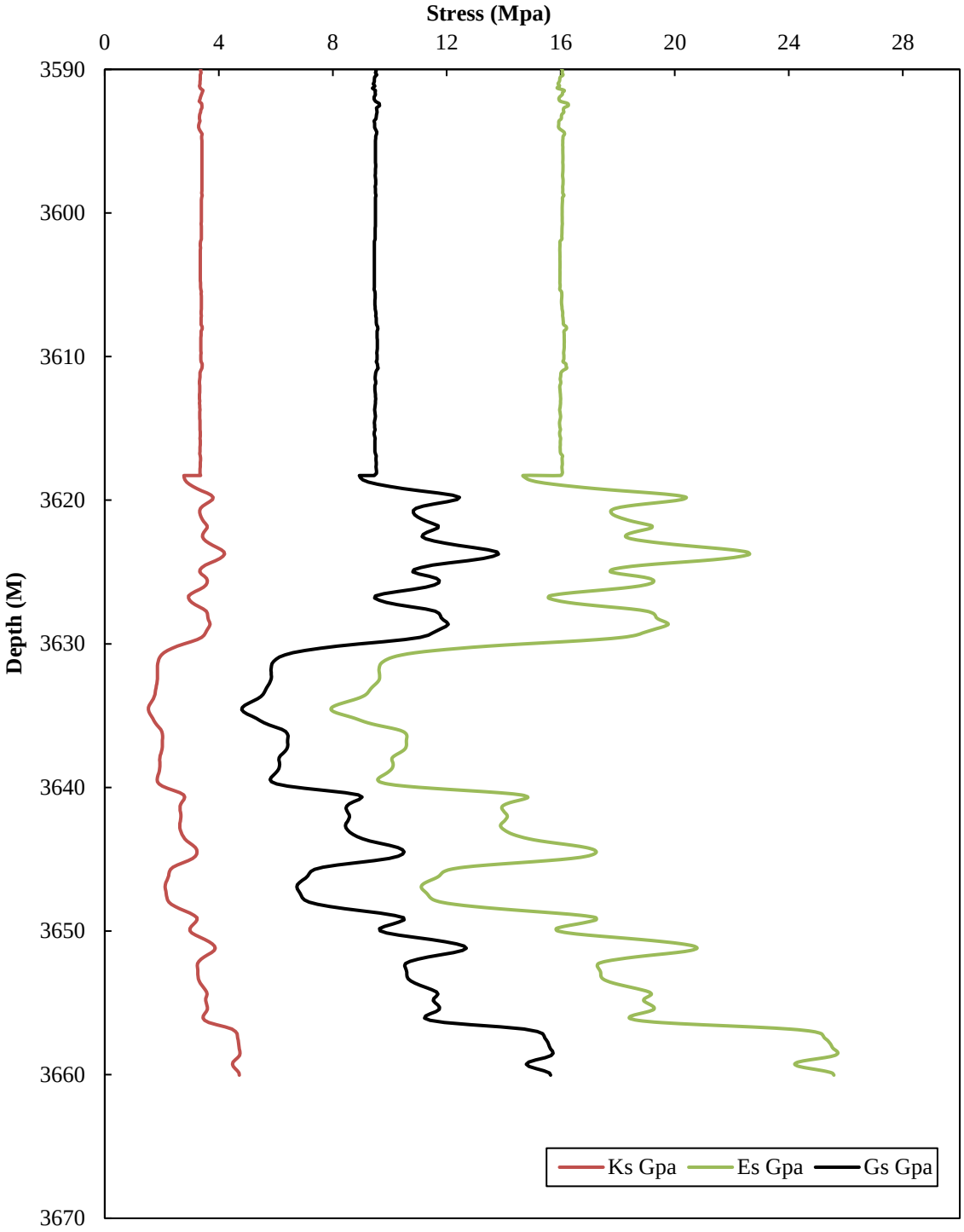

Figure 3

One-dimensional geomechanical model of static-elastic parameters of the cap rock.

Uniaxial compressive strength (UCS) is a major parameter in determining the range of variations of the main horizontal stresses. In 1998, Bradford introduced an equation based on the Young's modulus for the estimation of single-axial compressive strength (Goodman and Connolly, 2007):

$$UCS = 2.28 + 4.1089E_{sta} \quad (5)$$

4.2. Analysis of in situ stress field

The stress field consists of three components of vertical stress (S_v), minimum horizontal stress (S_{Hmin}), and maximum horizontal stress (S_{Hmax}), which are applied to the rock at a specific depth, perpendicular to each other. The rocks located deep below the ground are exposed to high levels of in situ stress. Vertical stress is due to the weight of the upper layers, which can be computed by using the overload density at each point (Zoback, 2007).

$$\sigma_v = \int_0^z \rho(z).g.dz \tag{6}$$

where, ρ is the rock density, and g is the earth gravity acceleration.

Pore pressure is the second property required to estimate the status of in situ stresses.

$$P_p = OBG - \left(OBG - P_{ng}\right) \times \left(\frac{DT}{DT_n}\right)^n \tag{7}$$

where, P_p is pore pressure, and OBG represents the gradient for increasing overload stress; P_{ng}, DT, and DT_n are hydrostatic pressure, the log of compressed sound waves, and normalized DT log respectively. n coefficient depends on the geological characteristics of the area in question.

In this study, the modular dynamics formation tester (MDT) results were used to determine the pore pressure of Asmari reservoir. The data of this experiment are point-and-point and indicate the pore pressure in the tested depth. In order to calculate pore pressure in Gachsaran formation, the following experimental relationship is used especially for the southwestern oil-rich regions of Iran.

$$P_P = -\left[(\sigma_V - P_{P_{hydro}}) \times \left(DT_N / DT\right)^3\right] + \sigma_V \tag{8}$$

$$DT_N = (-0.75 \times \sigma_V) + 140 \tag{9}$$

Also, a pro-elastic equation can be used as a preliminary estimate of horizontal and/or maximum stress in the field.

$$\sigma_H = \frac{\nu}{(1-\nu)}\left(\sigma_v - \alpha.P_p\right) + \alpha.P_p + \frac{E_{sta}}{(1-\nu^2)}\left(\varepsilon_y + \nu.\varepsilon_x\right) \tag{10}$$

$$\sigma_h = \frac{\nu}{(1-\nu)}\left(\sigma_v - \alpha.P_p\right) + \alpha.P_p + \frac{E_{sta}}{(1-\nu^2)}\left(\varepsilon_x + \nu.\varepsilon_y\right) \tag{11}$$

The terms ε_x and ε_y are strain components in x and y directions. Calculating and measuring these two components are a major challenge in the oil industry. Today, these coefficients can be calculated with the aid of a dipole (DSI) sound diagram which has different shear components. P_p represents the pore pressure of reservoir rock, and α is called the Biot's coefficient; $0 < \alpha < 1$, where:

$\alpha = 1$ for porous and permeable rocks like reservoir rocks;

$\alpha = 0$ for non-porous and impermeable rocks like cap rocks;

In the poroelastic method of estimating in situ stresses, first the extension components of linear strain on *x* and *y* axes are determined using Equations 12 and 13. In these equations, S_v is overload pressure, and *v* is Poisson ratio; *E*, ε_x, and ε_y represent Young's modulus, linear strain on *x* axis, and linear strain on *y* axis respectively.

$$\varepsilon_x = \frac{s_v \times v}{E} \times \left(\frac{1}{1-v} - 1\right) \tag{12}$$

$$\varepsilon_y = \frac{s_v \times v}{E} \times \left(1 - \frac{v^2}{1-V}\right) \tag{13}$$

In situ stresses are calculated for the studied reservoir and cap rock, and the result is presented in Figure 4.

To investigate the stress regime, Anderson's fault theory, as described below, is used:

Various stress or faulting regimes include the followings:

- Normal stress regime ($S_{v>}S_H>S_h$)
- Strike-slip stress regime ($S_H>S_v>S_h$)
- Reverse stress regime ($S_H>S_h>S_v$)

According to Figure 4, the stress regime in the study area is reverse fault system (compressional).

4.3. Calculation of the effect of stress buckling

If the mass reservoir is free, effective stress variations simply result from its expansion and contraction. However, in fact, reservoirs depend on the surrounding rocks that resist the tendency of the reservoir to expand and contract. Because of this conflict between internal driving forces and external constraints, anisotropic variations in total stress may be created depending on the geometry of the reservoir, the difference between the mechanical properties of the reservoir and those of the surrounding rocks, and the distribution of pore pressure in the reservoir. This phenomenon is called buckling (Fernández-Ibáñez, 2010). Based on the fact that changes in the size of horizontal stress inside or outside the reservoir can exist, the buckling ratios are defined to describe the general patterns of stress variation. The buckling ratios are more specific to poroelastic rocks. A linear relationship between stress and variation in pore pressure is defined by:

$$\gamma_H = \Delta\sigma_H \big/ \Delta P$$
$$\gamma_V = \Delta\sigma_V \big/ \Delta P \tag{14}$$

γ_H and γ_V are respectively horizontal and vertical buckling ratios; $\Delta\sigma_H$ and $\Delta\sigma_V$ are respectively horizontal and vertical stress change, and ΔP stands for the change in the pore pressure of the reservoir.

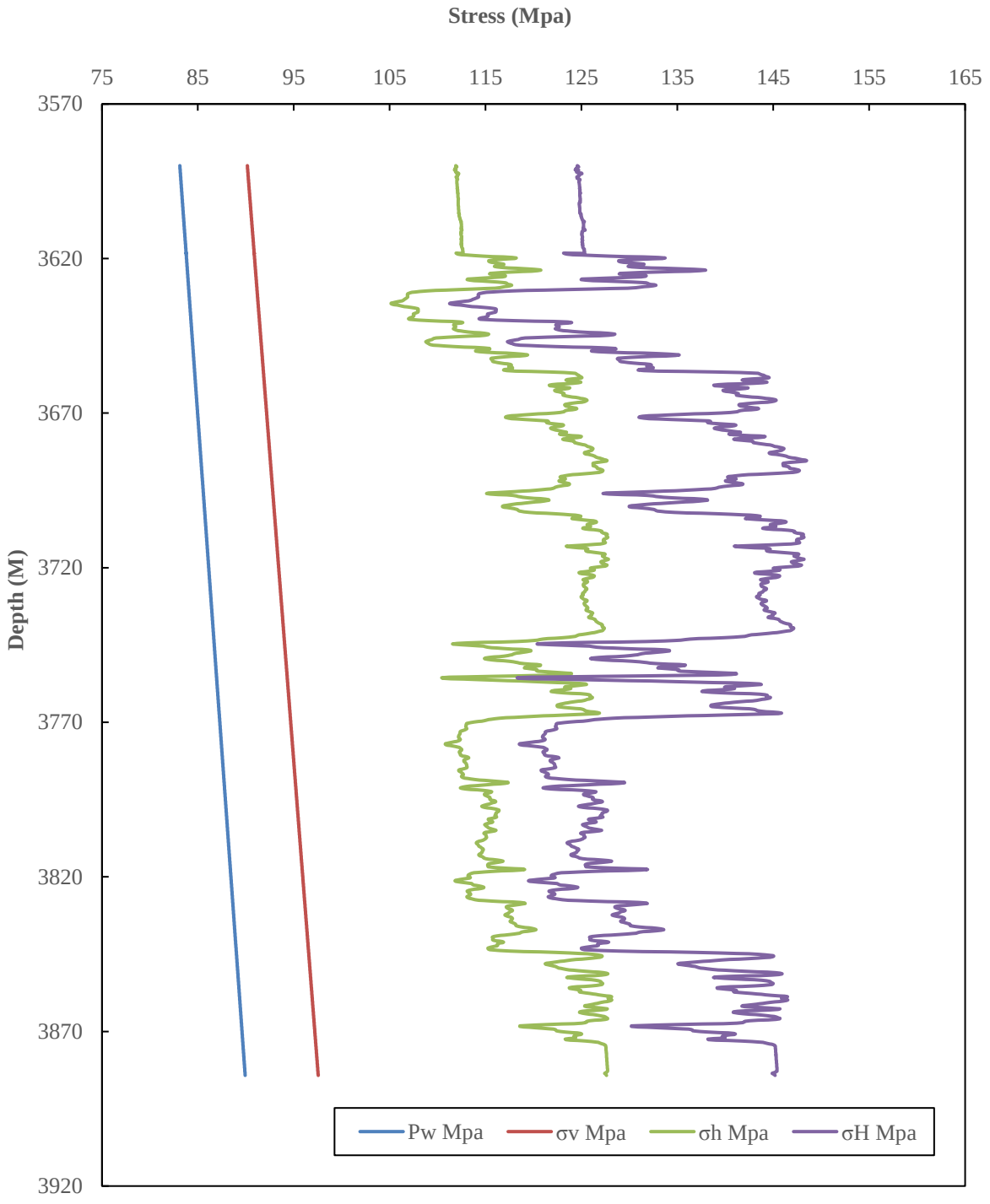

Figure 4

In situ stresses versus depth for cap rock and reservoir.

In this study, a more general form of this factor is defined as the ratio of effective pore pressure change inside the reservoir as follows ($\alpha\Delta P$: here α is Biot's coefficient, and ΔP is the pressure change in the reservoir that is positive during injection and negative during production):

$$\gamma_{\alpha(H_1)} = \Delta\sigma_{H_1} \Big/ (\alpha\Delta P)$$
$$\gamma_{\alpha(H_2)} = \Delta\sigma_{H_2} \Big/ (\alpha\Delta P) \quad (15)$$
$$\gamma_{\alpha(V)} = \Delta\sigma_{V} \Big/ (\alpha\Delta P)$$

Here, $\gamma_{\alpha(H_1)}$, $\gamma_{\alpha(H_2)}$, and $\gamma_{\alpha(V)}$ are respectively the normalized poroelastic, horizontal, and vertical buckling ratios. $\Delta\sigma_{H_1}$ and $\Delta\sigma_{H_2}$ are H1 and H2 stress variations. H_1 and H_2 represent the direction of two hypothetical parallel horizontal stresses (minimum and maximum in situ stresses).

These equations are referred to as coupling ratios due to the concept of effective stress and the relationship between pore pressure variations and their effects on stress field variations.

Using the proposed equations to calculate the magnitude of stresses and the Mohr-Coulomb criterion, the Moore circle was drawn to examine the state of production and/or injection. Figure 5 shows the Moore circle diagram for cap rock and reservoir rock in states where the rock material is homogeneous and heterogeneous.

In this calculation, it is also necessary to calculate the horizontal and vertical buckling parameters in relation to the overall shape. It should be noted that, in this study, because of the difference of mechanical properties of the reservoir with surrounding rocks, the heterogeneous theory was used. Also, for the overall shape of the reservoir, due to the relatively large length-to-width difference, an elliptical cylindrical reservoir was considered (Table 2).

Table 2

Calculation of buckling parameter with respect to the overall shape of the field.

Elliptic cylinder	$\gamma_{\alpha(H_1)} = \frac{1-2\upsilon}{1-\upsilon}\frac{1}{1+e}$ $\gamma_{\alpha(H_2)} = \frac{1-2\upsilon}{1-\upsilon}$ $\gamma_{\alpha(\upsilon)} = \frac{1-2\upsilon}{1-\upsilon}\frac{e}{1+e}$	$\gamma_{\alpha(H_1)} = A_1 \Big/ A_4.\gamma_{\alpha(H_2)} = A_2 \Big/ A_4.\gamma_{\alpha(\upsilon)} = A_1 \Big/ A_4$ $A_1 = (1-2\upsilon^*)\left[R_\mu[e(1-2\upsilon)+2(1-\upsilon)]+e\right]$ $A_2 = (1-2\upsilon^*)\left[R_\mu\left[R_\mu e(3-4\upsilon)+2(1+e^2)(1-\upsilon)\right]+e\right]$ $A_3 = (1-2\upsilon^*)\left[R_\mu[2e(1-\upsilon)+1-2\upsilon]+1]e\right]$ $A_4 = R_\mu\left[2(1+e)^2(1-\upsilon)(1-\upsilon^*) - 2e\upsilon^*(1-2\upsilon) + R_\mu e(3-4\upsilon)\right] + e(1-2\upsilon^*)$
Infinite Layer	$\gamma_{\alpha(H_1)} = \gamma_{\alpha(H_1)} = \frac{1-2\upsilon}{1-\upsilon};\ \gamma_{\alpha(\upsilon)=0}$	$\gamma_{\alpha(H_1)} = \gamma_{\alpha(H_1)} = \frac{1-2\upsilon^*}{1-\upsilon^*};\ \gamma_{\alpha(\upsilon)=0}$

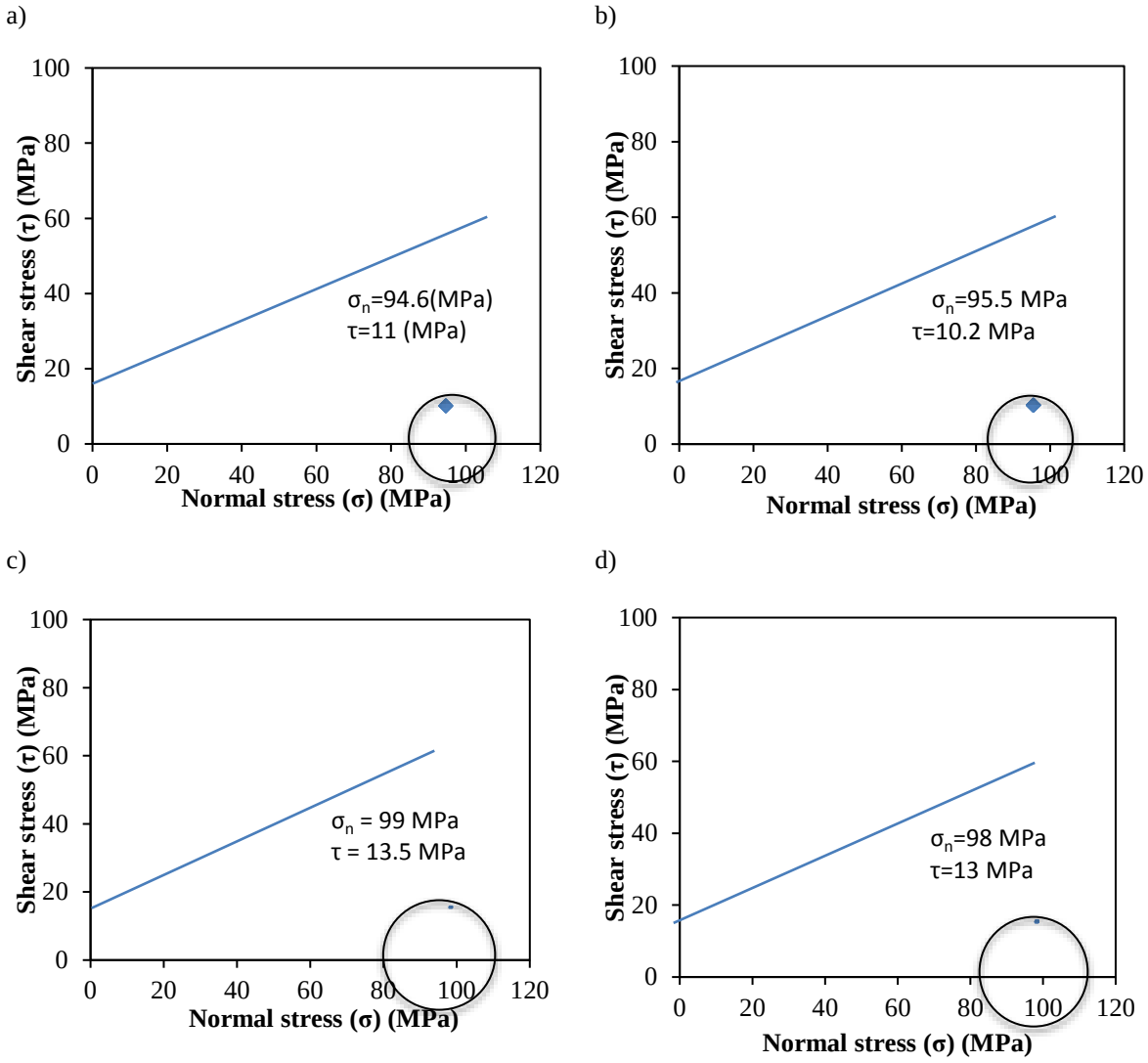

Figure 5

The Moore circle diagram: a) the cap rock in a homogenous state, b) the cap rock in a heterogeneous state, c) the reservoir in a homogenous state, and d) the reservoir in a heterogeneous state.

4.4. Reactivation of faults and their opening

The reactivation of faults at the time of injection depends on the design of injection pressure in the oilfield. When the pore pressure in the reservoir rises, normal stresses on the fault plane decrease; as a result, the fault is slipped and activated. By increasing the pore pressure, ultimately, the effective stresses reach zero and the faults open. The reactivation of faults and their openings prior to hydrocarbon transfer through porous layers to the surface is undetectable. Fault slip and reactivation were first normalized as one of the factors of fluid flow in fault zones by Sibson (1990) and based on the Mohr-Coulomb failure criterion; then, they were widely researched by Zubak (2007).

The reactivation of the faults was controlled by shear and normal stress components on the fault plane, which is shown below for a normal fault regime in two dimensions:

$$\tau = \frac{1}{2}(\sigma_V - \sigma_h)\sin(2\theta) \tag{16}$$

$$\sigma_n = \frac{1}{2}(\sigma_V + \sigma_h) + \frac{1}{2}(\sigma_V - \sigma_h)\cos(2\theta) \tag{17}$$

where, the slope is the fault, and the fault resistance behavior is based on the Mohr-Columbian criterion.

$$\tau_{slip} = C + \mu(\sigma_n - \alpha p) \tag{18}$$

where, p is pore pressure; α and C stand for Biot's coefficient and cohesion of the fault respectively. μ ($\mu = \tan\phi$) is the friction coefficient of fault for the friction fault angle of ϕ. In the above statement, $\sigma'_n = \sigma_n - \alpha p$ represents the normal stress on fault plane. The probability of reactivation for a fault is measured by the modified parameter of the fault tendency to slip.

$$ST = \frac{\tau}{\tau_{slip}} \tag{19}$$

ST is changing between zero and one. The higher the likelihood of fault slip is, the higher the likelihood of reactivation becomes.

Vertical stress strongly depends on the weight of upper layers. This stress component is less affected by reservoir pore pressure changes. In other words, the reservoir is limited in the horizontal direction, and the horizontal stress is influenced by the pore pressure. Based on Hills' research (2001), a change in the horizontal stress is inferred from production information and/or from the analysis of ideal reservoirs. During discharge, horizontal stress is reduced, so the difference in vertical and horizontal stresses is also increased; as a result, the fault is activated despite the increase of effective stresses as shown in Figure 6a. In this case, if the shear failure reaches the failure coating, the fault is reactivated. If normal effective stress reaches zero, the fault is opened, as shown in Figures 6b and 6c respectively.

There are two reverse faults in Marun field, which are created under the influence of increasing pressures on Iran and Saudi Arabia fault planes: one along the Marun anticline with a gradient varying by about 35° and the other along northwest-southeast with a gradient of 50°.

In Marun field, the occurrence of two major tectonic events, in the form of folding, caused by the effect of compressive forces and the continuation of orogenesis and deflection, have caused a great variety of slopes in anticline edges so far. Therefore, the radius of curvature across the construction is different in various sections.

In order to perform the analytical modeling of fault reactivation in the studied field, rock mechanics parameters derived from one-dimensional modeling were used.

The probability of the reactivation of faults No. 1 and No. 2 was also investigated as a representative of the field faults in depths. The results are listed in Tables 3 and 4.

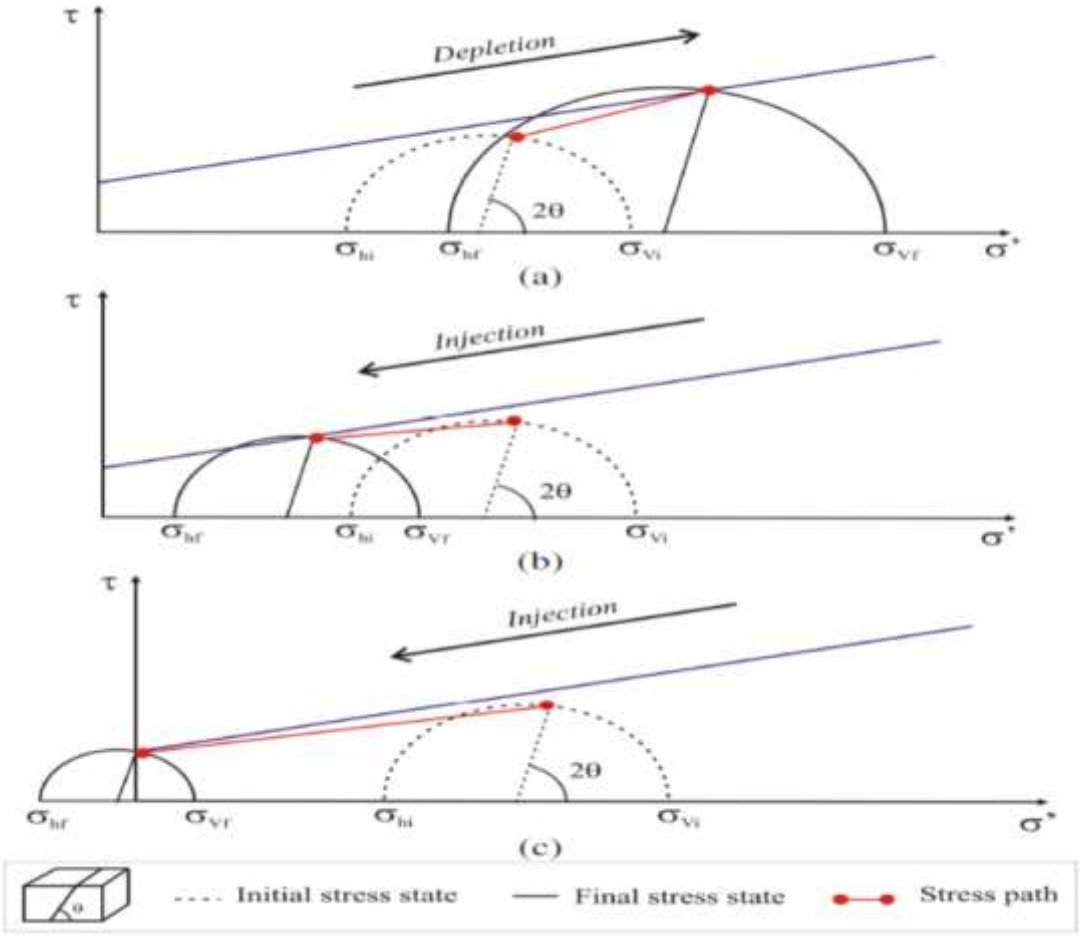

Figure 6

Mohr-Coulomb diagram: a) the activated fault at discharge time; b) the activated fault at injection time; and c) the opened fault at injection time.

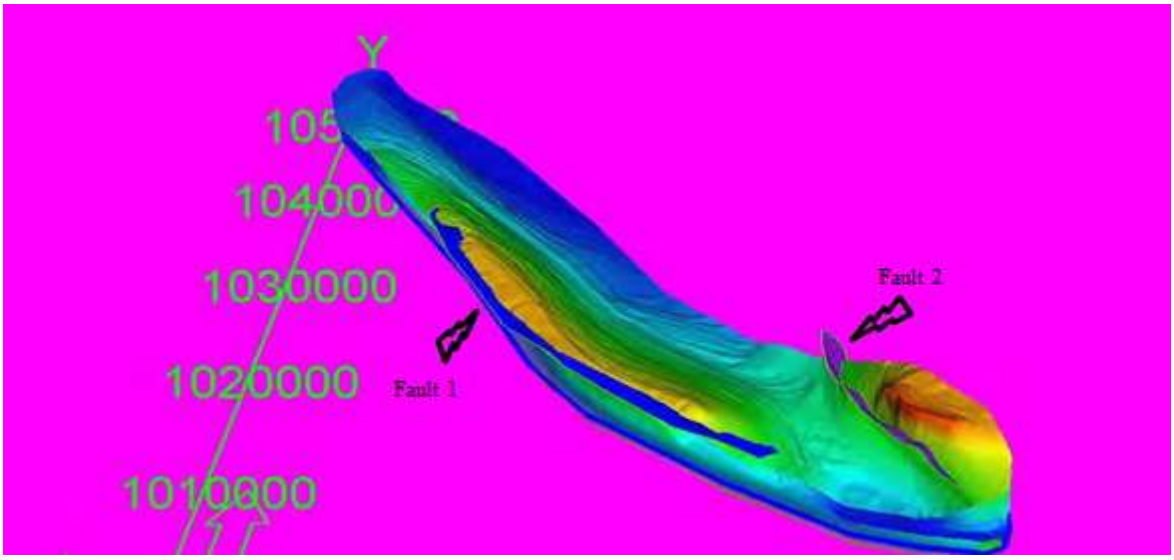

Figure 7

Three-dimensional image of a construction model derived from seismic data of Marun oilfield.

Table 3

The probability of reactivation of fault No. 1 in the current state of the reservoir pressure change.

Depth	V_s	τ Slip	UCS	P_p	σ_v	σ_H	C	θ	FRIC angle	A	μ	Δp (psi)	σ_n	τ-slip	ST
3590	0.18	14	68	99	90	124	16	35	39	1	0.6	1700	110	29	0.49
3600	0.18	15	68	100	90	124	16	35	39	1	0.6	1700	111	29	0.49
3630	0.21	10	62	100	91	123	14	35	39	1	0.6	1700	112	29	0.5
3640	0.21	13	54	101	91	120	13	35	38	1	0.6	1700	109	26	0.49
3650	0.21	15	69	101	91	126	15	35	40	1	0.6	1700	116	33	0.51
3660	0.22	22	96	101	91	139	20	35	44	1	0.6	1700	123	43	0.53
3700	0.21	16	75	102	92	130	16	35	41	1	0.6	1700	115	32	0.5
3750	0.21	16	74	103	94	131	16	35	41	1	0.6	1700	117	32	0.5
3780	0.21	11	49	104	94	121	12	35	36	1	0.6	1700	110	23	0.47
3820	0.21	21	45	105	95	120	11	53	36	1	0.6	1700	111	23	0.47
3870	0.22	19	85	106	97	139	18	35	43	1	0.6	1700	121	34	0.51

Table 4

The probability of reactivation of fault No. 2 in the current state of the reservoir pressure change.

Depth	V_s	τ Slip	UCS	P_p	σ_v	σ_H	C	θ	FRIC angle	α	μ	Δp (psi)	σ_n	τ-slip	ST
3590	0.18	15	68	99	90	124	16	50	39	1	0.6	1700	102	25	0.61
3600	0.18	15	68	100	90	124	16	50	39	1	0.6	1700	103	25	0.61
3630	0.21	14	62	100	91	123	14	50	39	1	0.6	1700	102	23	0.62
3640	0.21	12	54	101	91	120	13	50	38	1	0.6	1700	101	20	0.6
3650	0.21	15	69	101	91	126	15	50	40	1	0.6	1700	104	25	0.63
3660	0.22	21	96	101	91	139	20	50	44	1	0.6	1700	110	32	0.67
3700	0.21	17	75	102	92	130	16	50	41	1	0.6	1700	107	26	0.64
3750	0.21	17	74	103	94	131	16	50	41	1	0.6	1700	108	26	0.63
3780	0.21	11	49	104	94	121	12	50	36	1	0.6	1700	104	19	0.58
3820	0.21	10	45	105	95	120	11	50	36	1	0.6	1700	104	18	0.57
3870	0.22	19	85	106	97	139	18	50	43	1	0.6	1700	113	29	0.64

4.5. Induced fracture in the rock due to pressure change

The induced tensile and shear fracture of a reservoir and surrounding rocks during production time is responsible for the vibrational state recorded in many reservoirs in the world. In addition, it is classified as a major risk for the integrity of the reservoir and the cap rock during the fluid injection phase. Referring to Figure 8, it is clear that there are four different fracture modes during the pressure change in the reservoir: 1) horizontal tensile fracture ($\sigma'_V = 0$); 2) vertical tensile fracture ($\sigma'_H = 0$), 3) shear fracture in reverse fault stress regime (thrust fractures), and 4) shear fracture in normal fault regime (normal fractures).

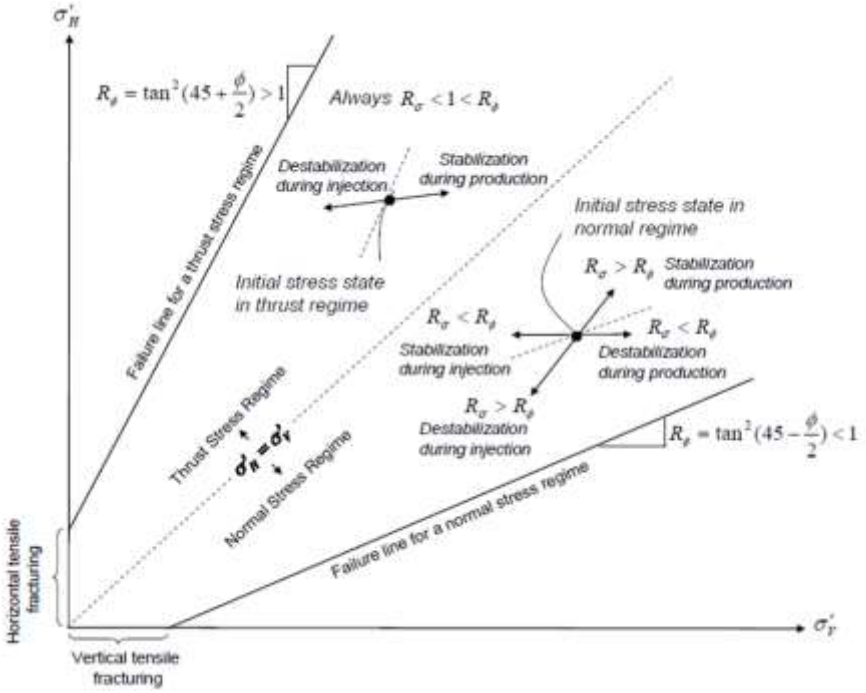

Figure 8

Demonstration of acceptable paths of stress variation at injection and production times for normal and reverse fault stress regimes (Zoback, 2007).

Equation 20 shows the critical pressure change $(\Delta P_f)_s$ in the reservoir rock. This stress change may result from production or injection. In this critical situation, the cutting takes place on the rock.

$$(\Delta P_f)_s/p_o = \frac{[K_o - \lambda_P] - [1-\lambda_P]R_\emptyset + 2C^*\lambda_P\delta_F\sqrt{R_\emptyset}}{\alpha\lambda_P\left(1-\gamma_{\alpha(V)}\right)[R_\sigma - R_\emptyset]} \tag{20}$$

A tensile fracture occurs if the critical pressure change is such that the effective stress is at least 0 or less. These conditions give rise to the following equations:

$$(\Delta P_f)_{T(H)}/p_o = \frac{(1-\lambda_P)}{\left[\alpha\lambda_P\left(1-\gamma_{\alpha(V)}\right)\right]} \tag{21}$$

Then, the graphs (Figures 9 and 10) of pressure changes during gas injection or production were drawn to produce induced shear and tensile fractures.

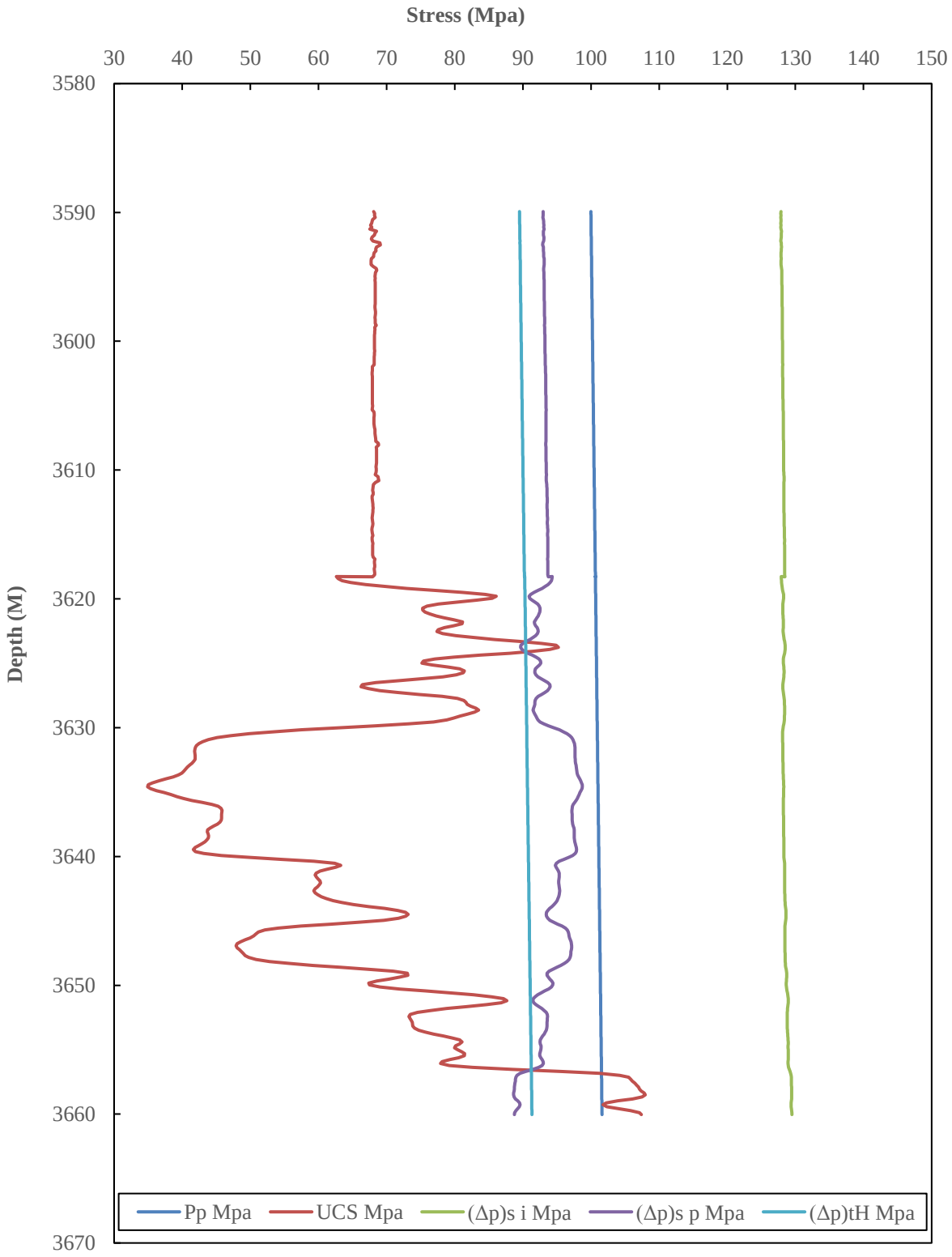

Figure 9

Critical pressure variation at injection and production times to create shear and tensile fractures in the cap rock.

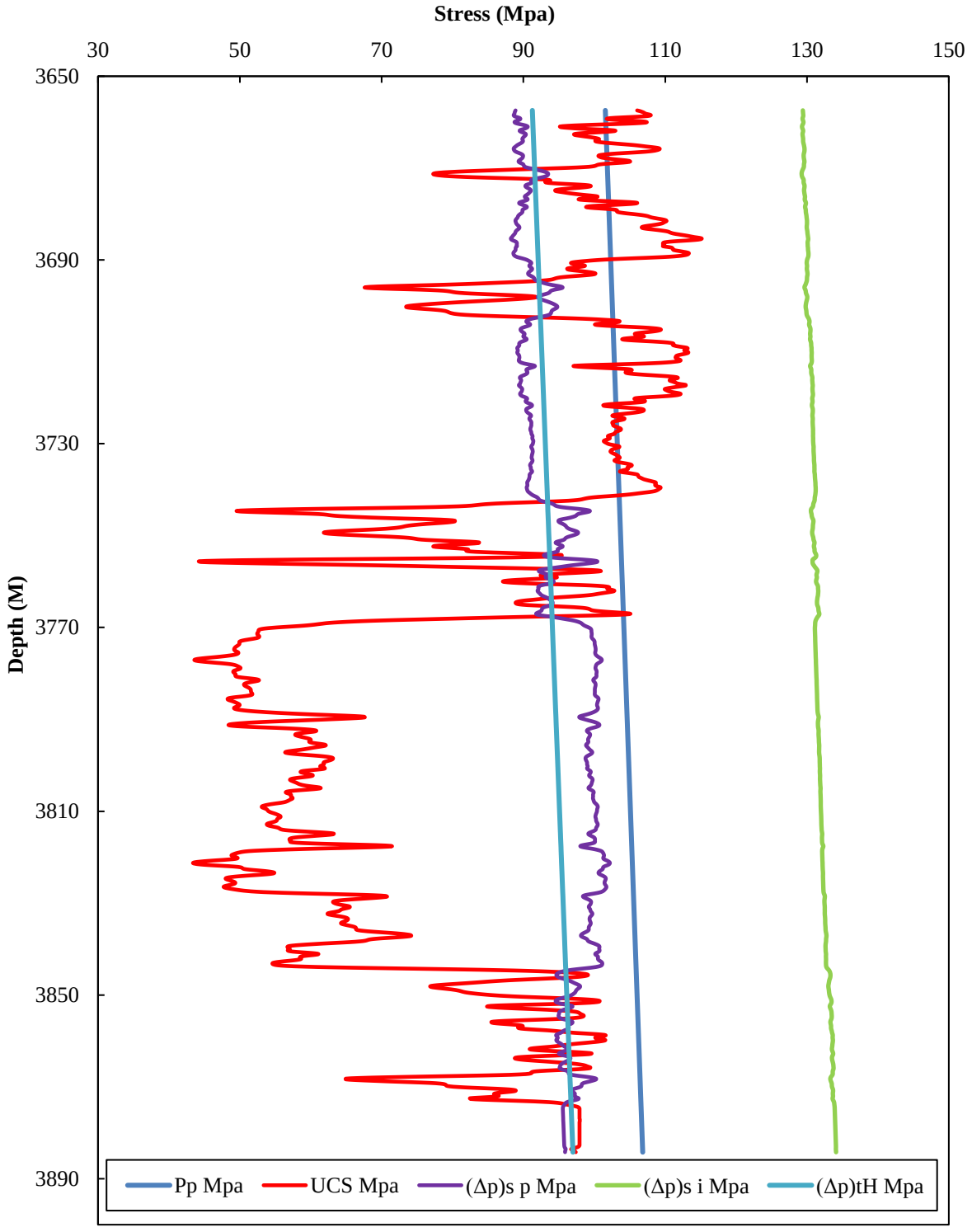

Figure 10

Critical pressure variation at injection and production times to create shear and tensile fractures in the reservoir rock.

4.6. Three-dimensional geomechanical modeling

ABAQUS was used for the numerical 3D modeling. ABAQUS is a collection of powerful engineering simulation programs based on the finite element method, which provides extensive capabilities for

simulation in linear and nonlinear applications (Koutsabeloulis and Xing, 2009). Matters with multiple components and different materials can be simulated by defining the geometry of each component, assigning its constituent material, and defining the interaction between these components. Figures 11 and 12 illustrate the three-dimensional modeling of rock and rock reservoirs respectively. These models can be carefully used to identify the places that have the greatest potential for deformation in these rocks.

In the 3D model, the geometric shape of the cap rock and reservoir was first designed. Then, stresses in the actual pressure state of the reservoir in the year studied (2018) were applied to the designed model. It should be noted that Asmari reservoir pressure in the field was 3400 psi in 2018. In the following, to analyze the strain and to study how to resist and integrate the cap rocks and reservoirs, the pressure gradually increases and decreases on the 3D model. The amount of pressure increase is based on the operation of the gas injection, and the amount of pressure reduction is based on the production history of the reservoir.

Finally, 3D modeling results show the amount of cap rock and reservoir resistance during injection and production processes, as shown in Figures 11 and 12. It should be noted that the process of connection between pore pressure and stresses in three-dimensional modeling has been one-way.

The coupling between the stress field and the reservoir pressure is considered on the basis of the operational process of gas injection, and the pressure reduction value is based on the production history of the reservoir.

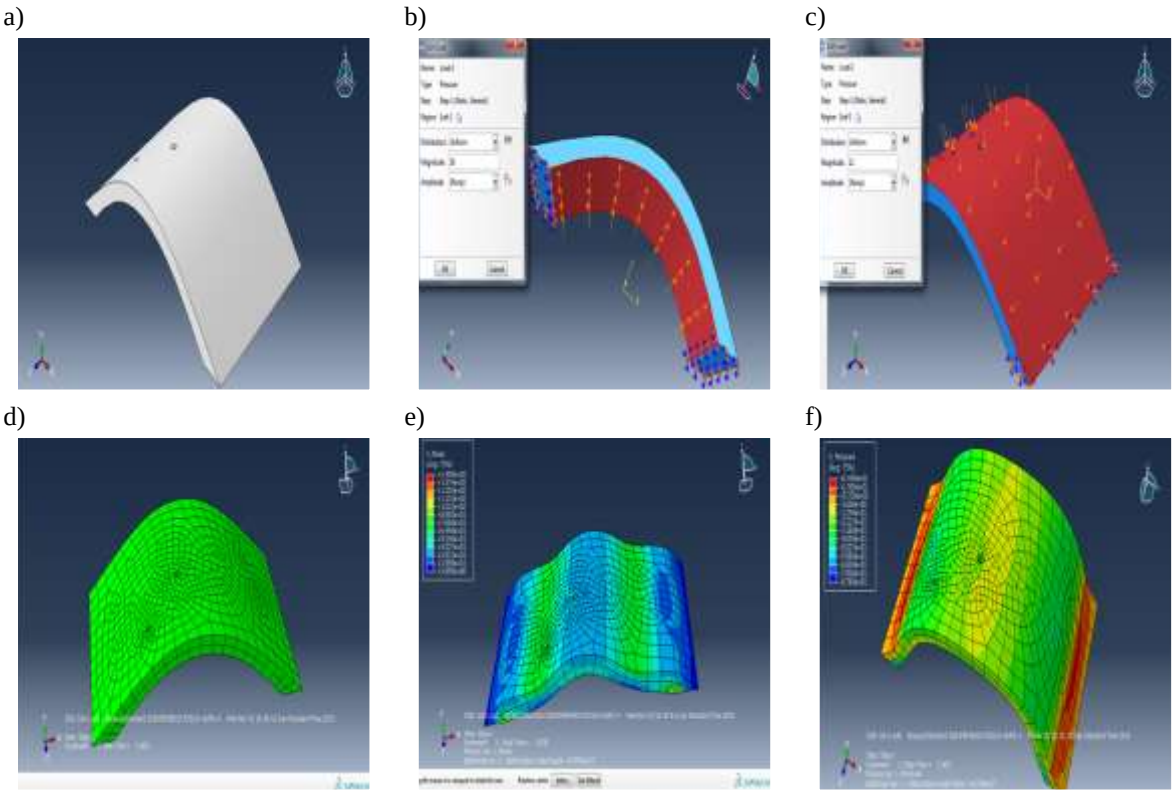

Figure 11

A 3D model of the cap rock designed in ABAQUS: a) model design; b) application of force to the cap rock (gas injection); c) application of force to the cap rock (production); d) cap rock meshing; e) changes caused by application of force to the cap rock (production); and f) changes caused by the application of force to the cap rock (gas injection).

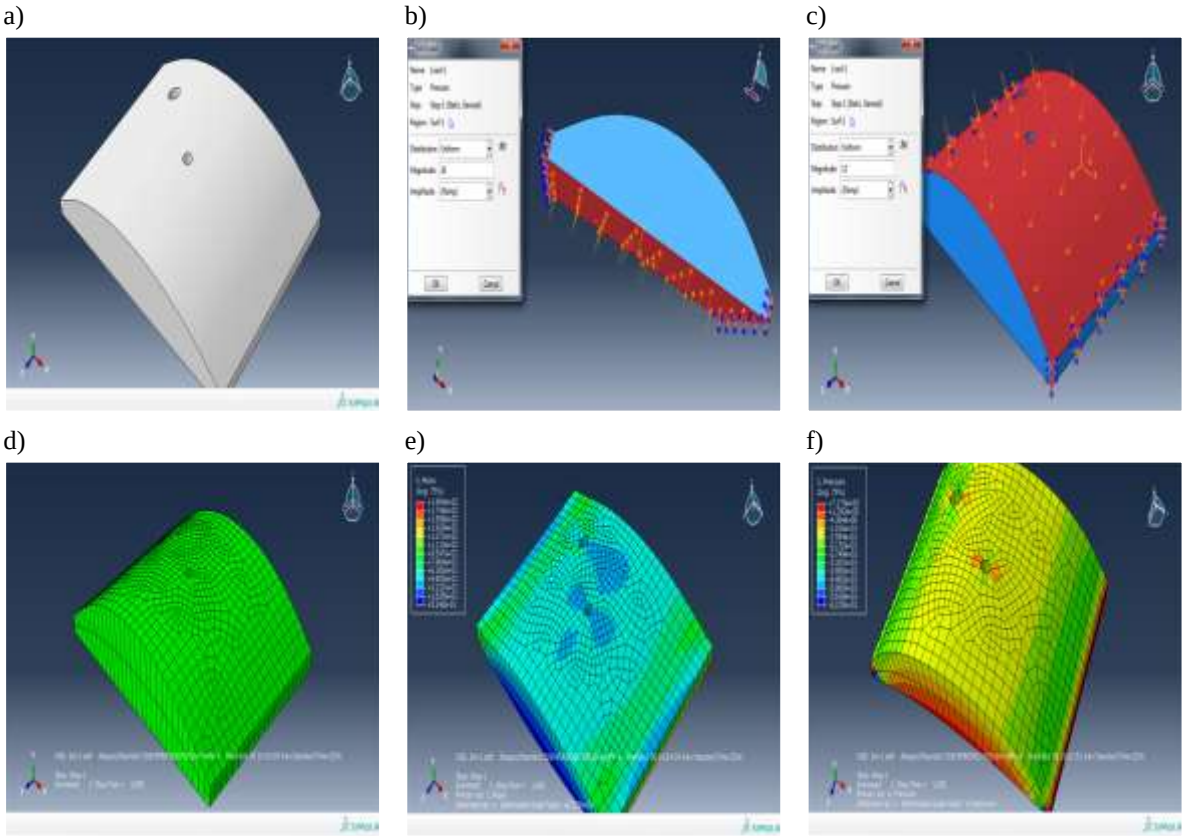

Figure 12

A 3D model of the reservoir designed in ABAQUS: a) model design; b) application of force to the reservoir (gas injection); c) application of force to the reservoir (production); d) reservoir meshing; e) changes caused by application of force to the reservoir (production); and f) changes caused by the application of force to the reservoir (gas injection).

5. Conclusions

In order to ensure the preservation of the integrity of impermeable boundaries (cap rocks, faults, etc.), it is necessary to conduct studies and geomechanical analyses during the production or injection in the reservoir. The integrity of impermeable boundaries may be threatened or destroyed by induced fractures or by the reactivation and/or reopening of the faults and fractures present on the boundaries. In general, the analysis and investigation of the issues and risks associated with gas injection from the geomechanical point of view include two major steps: first, the analysis of the amount of stress variation due to gas injection, and second, the analysis of the behavior of geological indicators (reservoir rock and cap rock layers, fractures, faults, etc.) caused by the induced stress. In total, for analyzing and modeling these stages, researchers have presented three different approaches, including numerical methods, semi-analytic methods, and analytical methods.

In the current work, by employing analytical and numerical methods, the following results were obtained:

1. Information from geomechanical models constructed in the wells of Marun oilfield, including the size of vertical stresses, and minimum horizontal stress, and the maximum horizontal stress indicates that an inverse fault regime is dominant in the field.

2. Using seismic sections obtained from three-dimensional geophysical surveys, two reverse faults were identified: one in the southern edge of the field along the anticline at an angle of about 35°, and another fault along the northwest-southeast at an angle of about 50°.
3. The tendency of the fault to slip is variable between zero and one. The measurements show the greater tendency of fault No. 2 towards reactivation compared to fault No. 1.
4. Critical pressure changes to produce tensile-induced fractures in injection and production phases are variable from 8 MPa (1160 psi) to 12 MPa (1740 psi) in cap rocks and reservoir rocks.
5. Critical pressure changes to produce induced-shear fractures in injection and production phases are variable from 26 MPa (3770 psi) (for injection) to -10 MPa (-1450 psi) (for production).
6. The lowest possible change in pressure was observed on the cap rock in a depth range of 3630 m to 3640 m with a change of pressure of about 1,000 psi.
7. The three-dimensional model designed shows that the most changes were around the wellheads, fractures, and edges of the field.

Nomenclature

P_p : Pore Pressure

ϑ : Poisson Ratio

S_v: Vertical Stress

S_{Hmin}: Minimum Horizontal Stress

S_{Hmax}: Maximum Horizontal Stress

E: Young's Modulus

γ: Buckling Ratios

ST: Fault Tendency to Slip

τ: Shear Stress

σ_n: Normal Stress

References

Abdideh M. and Hedayati Khah S., Analytical and Numerical Study of Casing Collapse in Iranian Oil Field, Geotechnical and Geological Engineering, Vol. 36, p. 1723-1734, 2018.

Afsari M., Ghafoori M.R., Roostaeian M., Haghshenas A., Ataei A., and Masoudi R., Mechanical Earth Model (MEM): An Effective Tool for Borehole Stability Analysis and Managed Pressure Drilling (Case Study), the 2009 SPE Middle East Oil & Gas Show and Conference, Bahrain: Society of Petroleum Engineers, p. 1-12, 2009.

Akbar A., Watching Rocks Change Mechanical Earth Modeling, Oilfield Review, Houston, Texas, USA: Schlumberger, 2005.

Ansari S., Haigh R., Khosravi N., Khan S., Han H., and Vishteh M., Cap rock Integrity Case Study for Non-thermal Polymer Flooding Project Using 4D Reservoir Coupled Geomechanical Simulation, the SPE Heavy Oil Conference,12–14 June, Calgary, Alberta, Canada: Society of Petroleum Engineers, p. 1-15, 2012.

Archer S. and Rasouli V., A log-based Analysis to Estimate Mechanical properties and in-situ Stresses in a Shale Gas Well in North Perth Basin, Petroleum and Mineral Resources, Vol. 21, p. 122-135, 2012.

Assef M.H., Minton J., Rawnsley K., Qiuguo L., Zhang X., and Koutsabeloulis N., Coupled Reservoir Geomechanical Modeling of a Thermal Gas-Oil-Gravity-Drainage Project, the Conference at Oil & Gas West Asia,11–13 April , Muscat, Oman: Society of Petroleum Engineers, p. 1-12, 2010.

Chang C. and Zoback M., Empirical Relations between Rock Strength and Physical Properties in Sedimentary Rocks, Journal of Petroleum Science and Engineering, Vol. 51, p. 223–237, 2006.

Dipankar D., A 3D Coupled Reservoir Geomechanics Study for Pressure, Water Production, and Oil Production Simulation: Application in Umm-Gudair Field, West Kuwait, the SPE Reservoir Characterization and Simulation Conference and Exhibition, Abu Dhabi, UAE: Society of Petroleum Engineers, p. 7-17, 2011.

Eissa A. and Kazi A., Relation between Static and Dynamic Young's Moduli of Rocks, International Journal of Rock Mechanics and Mining Sciences, Vol. 34, p. 479 – 482, 1988.

Fernández-Ibáñez, F., 3D Geomechanical Modeling for the Apiay and Suria Oil Fields (Llanos Orientales Basin, Colombia): Insights on the Stability of Reservoir Bounding Faults, The SPE Latin American & Caribbean Petroleum Engineering Conference, Lima, Peru: Society of Petroleum Engineers, p. 1-14, 2010.

Fjaer E., Holt R.M., Horsrud P., Raaen A.M., and Risnes R., Petroleum Related Rock Mechanics, Hungary: Elsevier, 2008.

Goodman H .E., Connolly P., Reconciling Subsurface Uncertainty with the Appropriate Well Design Using the Mechanical Earth Model (MEM) Approach, International Petroleum Technology Conference, 4-6 December, Dubai, U.A.E., p. 5-14, 2007.

Han H., Khan S., Ansari S., and Khosravi N., Prediction of Injection Induced Formation Shear, the SPE International Symposium and Exhibition on Formation Damage Control, 15–17 February, Lafayette, Louisiana, USA, p. 1-10, 2012.

Holland M., Brudy M., van der Zee W., Perumalla S., and Finkbeiner T., Value of 3D Geomechanical Modeling in Field Development: A New Approach Using Geostatistics. SPE/DGS Annual Technical Symposium and Exhibition, 4-7 April, Al-Khobar, Saudi Arabi, p. 1-7, 2010.

Khaksar A.P.G., Taylor Z., Fang, T., Kayes A., Salazar, and Rahman k., Rock Strength from Core Logs: Where We Stand and Ways to Go, EUROPEC/EAGE Annual Conference and Exhibition, 8-11 June, Amsterdam: Society of Petroleum Engineers, p. 2-8, 2009.

Koutsabeloulis N. and Xing Z., 3D Reservoir Geomechanical Modeling in Oil/Gas Field Production, SPE Saudi Arabia Section Technical Symposium and Exhibition, 9-11 May, AlKhobar, Saudi Arabia, p. 1-14, 2009.

Lee D.W., Quantifying Reservoir Compaction in an Unconsolidated Pliocene Reservoir Using Time-Lapse Seismic, Continuous Downhole Pressure Monitoring, and 3D Finite Element Modeling, 47th US Rock Mechanics/Geomechanics Symposium, 23-26 June, San Francisco, CA, USA: American Rock Mechanics Association, p. 1-9, 2013.

Luiz Serra de Souza A., Reservoir Geomechanics Study for Deepwater Field Identifies Ways to Maximize Reservoir Performance While Reducing Geomechanics Risks, SPE Asia Pacific Oil

and Gas Conference and Exhibition, 22-24 October, Perth, Australia: Society of Petroleum Engineers, p. 1-19, 2012.

Perfetto R., Fracture Optimization Applying a Novel Traceable Proppant and a Refined Mechanical Earth Model in the Congo Onshore, the International Petroleum Technology Conference, 26–28 March, Beijing, China, International Petroleum Technology Conference, p. 1-12, 2013.

Rivero J.A., Modeling CHOPS Using a Coupled Flow-geomechanics Simulator with Nonequilibrium Foamy-Oil Reactions: A Multi-well History Matching Study, the SPE Annual Technical Conference and Exhibition, 19-22 September, Florence, Italy: Society of Petroleum Engineers, p. 1-21, 2010.

Zoback Mark D., Reservoir Geomechanics, New York, United States of America: Cambridge University Press, 2007.